Macromolecules
ARTICLE

Macromolecules **2010**, *43*, 9371–9375 **9371**
DOI: 10.1021/ma102188d

Efficient Approaches for the Surface Modification of Platinum Nanoparticles via Click Chemistry

Eric Drockenmuller,[‡] Isabelle Colinet,[†] Denis Damiron,[‡] François Gal,[†] Henri Perez,[§] and Géraldine Carrot*[,†]

[†]*Laboratoire Léon Brillouin (CEA/DSM/IRAMIS/LLB-CNRS), Bâtiment 563, CEA/Saclay, 91191 Gif-sur-Yvette, France,* [‡]*Université Claude Bernard Lyon 1, CNRS, Ingénierie des Matériaux Polymères, 69622, Villeurbanne, France, and* [§]*Laboratoire Francis Perrin (CEA/DSM/IRAMIS/SPAM-CNRS), Bâtiment 522, CEA/Saclay, 91191 Gif-sur-Yvette, France*

Received September 21, 2010

ABSTRACT: Hybrid nanoparticles based on platinum nanoparticles (PtNPs) are of great interest for applications in fuel cells or as biosensors. Polymer chains covalently attached to the PtNPs may improve both the (bio)compatibility, solubility, and stability of the PtNPs, without inhibiting their electrochemical properties. First, we performed a copper(I)-catalyzed azide−alkyne cycloaddition (CuAAC) "grafting to" method to graft either poly(ethylene glycol) (PEG) or poly(ε-caprolactone) (PCL) onto PtNPs to create new hybrid nanoparticles with a biocompatible corona. Second, we combined both *surface*-atom transfer radical polymerization "grafting from" copolymerization of azide-functionalized monomers and CuAAC "grafting to" coupling of PEG or PCL to construct more complex polymer architectures. These approaches afforded a large library of nanostructures with varying chemical nature, microstructure, radius, and morphology of the polymer corona. Infrared spectroscopy, thermogravimetric analysis, and more detailed SANS experiments proved that these methodologies are simple, efficient, and wide in scope for the preparation of highly functional metal nanoparticles with tunable properties.

Introduction

Platinum nanoparticles (PtNPs) are of significant importance in applications such as fuel cells or biosensors due to their peculiar catalytic and conductive properties which are guided by their specific surface area.[1,2] The covalent tethering of polymer chains to tailor-made functionalized PtNPs is a particularly robust approach to improve the compatibility, the solubility, and the stability of these polymer/platinum nano-objects. Grafting of tailored polymer chains onto nanoparticles has been explored using the "grafting from" polymerization method,[3a] relying on *surface*-atom transfer radical polymerization (*surface*-ATRP).[3] We found out that this versatile approach was efficient for the functionalization of PtNPs,[4c,d] without any need for sacrificial initiator in the polymerization media as a consequence of the high specific surface area of such NPs. We have particularly showed before that the electrochemical properties of the Pt core were not inhibited by the organic corona,[4e,f] although the latter greatly enhanced their 2D organization as Langmuir−Blodgett thin films[4b,d] or cross-linked multilayer assemblies.[4g] Such nanostructures offer large perspectives as both platinum core and organic corona properties may be exploited. Now, we wanted to go further in the design of a biocompatible and water-soluble polymer corona with the objective of constructing biosensors. However, the main limitations of *surface*-ATRP are its exclusive application to vinyl monomers and the difficult access to the molecular characteristics of the grafted polymer chains. On the contrary, the "grafting to" approach has the advantage of known parameters of the grafted polymer precursors, with a larger range of polymers potentially reacting. However, its disadvantages are the poor control over grafting density and a lack of chemical orthogonality.

*Corresponding author. E-mail: geraldine.carrot@cea.fr.

Therefore, there is a strong driving force to explore new robust and efficient grafting approaches to tailor the properties of PtNPs. Particularly, tethering of biocompatible polymers, such as poly(ethylene glycol) (PEG) or poly(ε-caprolactone) (PCL) that are not compatible with ATRP conditions, is highly desirable when considering bioapplications.[2] In this scope, the concept of click chemistry recently introduced by Sharpless and Meldal is particularly attractive.[5] So far, the most studied and reliable example of this concept is the copper(I)-catalyzed azide−alkyne cycloaddition (CuAAC) which yields exclusively 1,4-disubstituted 1,2,3-triazoles. This reaction has many advantages that have attracted the polymer chemist community, e.g., high efficiency, tolerance to a wide range of functional groups and reaction media, and mild processing conditions in protic or aprotic solvents.[6] Several studies have shown that CuAAC reaction is a particularly appropriate method for the functionalization of 2D and 3D (in)organic substrates.[7] The surfaces of e.g. silica[7e−g] and gold[7i] nanoparticles have been previously decorated using CuAAC, but the grafting of PtNPs has not been addressed before. Note that the sizes of the metal particles are similar (2−3 nm in diameter), but surface chemistry of platinum is different than gold due to the strong affinity of Pt with sulfur, leading to an irreversible binding of the ligands or polymers.

Most drawbacks of standard "grafting to" approaches have thus been offset by the strong efficiency of the CuAAC process. We present herein CuAAC-based grafting approaches for the versatile and efficient functionalization of PtNPs. These approaches are based on tailor-made azide-functionalized PtNPs and alkyne-functionalized linear brush precursors. We also extended the possibilities by combining both "grafting from" (*surface*-ATRP) and "grafting to" (click chemistry) methods to improve the complexity and the density of the polymer corona, as shown in previous work on 100 nm silica NPs (combination of

Published on Web 10/20/2010

surface-RAFT and click chemistry).[7g] The efficiency of these grafting approaches has been validated by the precise determination of the organic corona characteristics (amount of grafted polymer, efficiency of the reaction, grafting density) obtained from thermogravimetric analysis, and more detailed studies of the afforded structures have been performed from small-angle neutron scattering (SANS).

Experimental Section

Materials. Bromine-functionalized platinum nanoparticles (Br-PtNPs) were obtained following a previously described method.[4a,d] Azide-modified methacrylate and α-methoxy-ω-ethynyloxy-poly(ethylene glycol) were synthesized according to already published procedures.[8a,b] Monomers have been distilled over calcium hydride or filtered through neutral alumina. All other reactants were purchased from Aldrich and used as received.

Characterization. ^{1}H NMR spectra were recorded on a Bruker 400 MHz in $CDCl_3$. Thermogravimetric analysis (TGA) was performed on a TA Instruments Q50, at a scan rate of 20 °C/min, up to 800 °C under air. Differential scanning calorimetry (DSC) was performed on a TA Instruments DSC Q100, at a scan rate of 10 °C/min. Infrared spectra were recorded on a Perkin-Elmer FTIR spectrometer using KBr pellets. Transmission electron microscopy (TEM) images were recorded on films solvent-casted onto carbon grids, using a Philips CM12 (120 keV) transmission electron microscope.

Small-angle neutron scattering (SANS) experiments have been performed on the PACE and PAXE spectrometers (Laboratoire Léon Brillouin, Saclay). Three configurations (wavelength λ_0 = 6.0 Å, $D_{\text{sample-to-detector}}$ = 1 and 4.57 m) were used, covering a q range of 0.004−0.31 Å^{-1}. Data treatment was done with a homemade program (PAsiNET, LLB) following standard procedures,[9] with H_2O as calibration standard. Incoherent background was determined with several H/D mixtures and interpolated for the desired concentrations. The absolute values of the scattered intensity (in cm^{-1}) were measured via a determination of the direct beam intensity. Experiments have been performed in a mixture of 95.7% of deuterated dimethylacetamide (d_9-DMAc) and 4.3% of hydrogenated DMAc because the scattering length density (index matching) value ($\rho_{d_9\text{-DMAc}} = 6.6 \times 10^{10}$ cm^{-2}) of this solvent is close to the one of the platinum core ($\rho_{\text{Pt}} = 6.3 \times 10^{10}$ cm^{-2}) and sufficiently far from the polymer one ($\rho_{\text{PEG}} = 0.62 \times 10^{10}$ cm^{-2}). This value (95.7% of d_9-DMAc and 4.3% of hDMAc) permitted to match exactly the contribution of the platinum core and to increase the intensity of the signal due to the polymer corona. Samples have been studied and prepared at a concentration of roughly 6 mg/mL, which corresponds to a volume fraction of polymer of 0.5% (the platinum volume fraction is 4×10^{-3}%).

Synthesis and Characterization of "Clickable" Precursors. *General Procedure for the Surface-Atom Transfer Radical Polymerization* (*Surface-ATRP*). Bromoisobutyryl-modified PtNPs (Br-PtNPs) in DMAc (5 mg/mL, with roughly 20%wt of bromine moieties), Cu^IBr, and PMDETA were mixed in a three-neck flask under nitrogen. The Cu^IBr/PMDETA/initiator molar ratio was 2:3:1. The reaction mixture was stirred until it became homogeneous. The monomers (chloromethylstyrene/styrene (CMS/Sty) or azide-modified methacrylate/butyl methacrylate (N_3MA/BuMA)) were added in various ratios (25:75 or 50:50), and the reaction mixture was heated to 60 °C (for methacrylate) or 110 °C (for styrene). The catalyst-to-monomer molar ratio was 0.005 for a theoretical molecular weight of 50 000 g mol^{-1}. The reaction was stirred for 5 h under an inert atmosphere. The afforded polymer-*grafted*-PtNPs were precipitated from a diethyl ether/ethanol (70/30) mixture. Kinetic samples were taken via purged syringes and were used to determine conversion by gravimetry (see Supporting Information). The evolution of the kinetic plots was quasi-linear, thus attesting for the good control of the copolymerization. No strong difference is observed in the kinetics of the copolymerization for the different ratios of CMS/styrene, even compared to the *surface*-ATRP of styrene. The polymer-to-platinum ratio was determined from TGA (see Supporting Information for details of calculation).

General Procedure for Azidation of the PtNPs. Synthesis of Azide-Modified PtNPs (*N_3-PtNPs*) *and Azide-Modified Polymer-g-PtNPs* (*PSN_3-g-PtNPs*). Styrene/chlorostyrene copolymer-*grafted*-PtNPs (PSCl-*g*-PtNPs) (1 equiv) or Br-PtNPs (1 equiv) were dissolved in a saturated solution of NaN_3 (4 equiv) in DMF, and the solution was stirred at 40 °C for 12 h. The particles were recovered by precipitation in water followed by several centrifugation/dispersion cycles at 4000 rpm for 5 min. In both cases, infrared spectra showed the characteristic signal of the azide groups at 2097 cm^{-1} (see Figures S1 and S2 in the Supporting Information). Moreover, in the case of the PSN_3-*g*-PtNPs, we can also see the quasi-complete disappearance of the chloride groups with the C−Cl stretching at 824 cm^{-1} after the conversion to azide groups.

Synthesis of the ω-Alkyne-Terminated PCL. Poly(ε-caprolactone) (PCL) of 900 and 3000 g/mol were synthesized from ring-opening polymerization (ROP) with benzyl alcohol/aluminum isoproxide for initiation.[8c] A solution of DCC (0.38 g, 1.5 equiv) was added dropwise to a stirred solution of PCL (1 g, 1 equiv) in 10 mL of CH_2Cl_2 followed by the addition of 4-pentynoic acid (0.246 g, 2 equiv) and (dimethylamino)-pyridine (DMAP) (0.3 equiv). The reaction mixture was stirred at room temperature for 24 h, before being filtered and evaporated. The crude product was purified by three consecutive precipitations in cold heptanes, and ω-alkyne−PCL was obtained as a white solid. The presence of the alkyne group was confirmed by ^{1}H NMR by a signal at 2.5 ppm corresponding to the proton (−C≡C*H*) of the terminal acetylene moieties. The infrared spectrum of the crude product shows the presence of a sharp peak at 3326 cm^{-1}, characteristic of the alkyne groups.

^{1}H NMR spectrum of ω-alkyne−PCL in $CDCl_3$. δ (ppm): 7.35 (s, C_6H_5, 5H); 5.10 (s, C_6H_5−CH_2−, 2H); 2.32 (t, −O−CH_2−CH_2−, 2H); 1.59−1.71 (m, −OCH_2−CH_2−CH_2−, 4H); 1.41−1.32 (m, −$CH_2C H_2CH_2$−, 2H); 4.02−4.12 (m, −CH_2−CH_2−O−, 2H); 1.02−1.20 (m, −OCO−CH_2−CH_2, 2H); 1.94 (t, −$CH_2C H_2$−C≡CH, 2H); 2.53 (t, −CH_2−C≡C*H*, 1H). All infrared spectra of the polymer precursor are given in the Supporting Information, together with the "clicked" products.

Synthesis and Characterization of the "Clicked" Polymer-*grafted*-PtNPs. The general conditions for the CuAAC reaction between N_3-PtNPs (or PSN_3-*g*-PtNPs, or $PBMAN_3$-*g*-PtNPs) with ω-alkyne-PEG (or ω-alkyne-PCL) are given below.

N_3-PtNPs (15 mg, 1 equiv of N_3 functionalities) were dissolved in DMAc (10 g/L) followed by the addition of the functional ω-alkyne polymers (0.154 g, 1 equiv) and CuBr (2 equiv). The reaction medium was degassed, stirred, and left under nitrogen before the addition of PMDETA (3 equiv). The mixture was stirred at 40 °C for 48 h under an inert atmosphere, and the reaction was stopped by cooling with ice. The "clicked"-modified PtNPs were precipitated in water or ether, and collected through centrifugation at 4000 rpm for 5 min. The cycle of centrifugation/redispersion in water was repeated three times to remove any residual copper bromide. The polymer-*grafted*-PtNPs were finally collected and subjected to repeated cycles of precipitation in acetonitrile followed by centrifugation to remove the nonreacted ω-alkynes polymer precursors (PEG and PCL). The polymer-*grafted*-PtNPs were dried at room temperature, in vacuum for 24 h before further characterization. These objects have been mainly characterized by TGA and FTIR before a more detailed SANS study. All the infrared spectra of the intermediates and products are summarized below. The decrease of the azide stretch (2096 cm^{-1}) from the clickable PtNPs (or polymer-*grafted*-precursors) after CuAAC reaction indicates the covalent attachment of the PCL (or the PEG) chains. The emerging strong absorption band located at 1736

and 1186 cm^{-1} (PCL/PS-*g*-PtNPs spectrum) is assigned to the carbonyl of the ester group of PCL grafts. Finally, the absence of alkyne stretching in the latter infrared spectra (see Figures S3−S5 in the Supporting Information) confirms the efficiency of the purification step and thus the absence of nonreacted PCL or PEG chains.

Results and Discussion

CuAAC "Grafting To" Route. A first strategy consists in the CuAAC grafting of ω-alkyne linear polymers to PtNPs having azide functionalities at their surface (Scheme 1).

Therefore, tailor-made PtNPs having bromide functionalities at their surface (Br-PtNPs) were converted to azido-functionalized PtNPs (N_3-PtNPs) by substitution of the bromide atoms by sodium azide (NaN_3) in dimethylacetamide (DMAc). In parallel, ω-alkyne PCL ($M_n \sim 0.9$ and 3 kg/mol) and PEG ($M_n \sim 5$ kg/mol) were respectively obtained by esterification of PCL with pentynoic acid and alkylation of monomethoxy-PEG with propargyl bromide. Then, the CuAAC "grafting to" process was performed using CuBr/PMDETA as the catalytic system in DMAc for 24 h, at room temperature under nitrogen.

Scheme 1. Synthesis of Hybrid PtNPs via the CuAAC "Grafting To" Approach

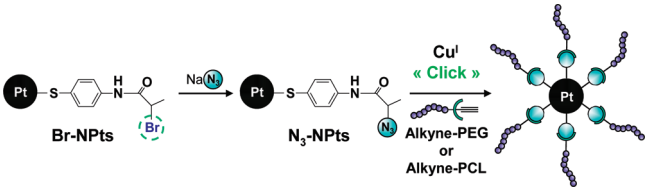

After purification by centrifugation to extract both nonreacted chains and residual catalytic system, polymer-*grafted*-PtNPs were recovered as non-aggregated and redispersible black powders (PCL-*g*-PtNPs and PEG-*g*-PtNPs). Thermogravimetric analysis (TGA) permitted to accurately quantify the increase in organic content after the CuAAC grafting of end-functionalized polymer precursors (Table 1).

Both grafting rates and grafting densities of the resulting hybrid PtNPs have been calculated from the organic content obtained from TGA (see Supporting Information for calculation details). As expected, they both decrease with the increase in molecular weight (M_n) of the "clicked" polymer chains as a result from the steric hindrance of the neighboring grafted chains. Nevertheless, grafting densities ranging from 0.9 to 1.8 chains/nm^2 were obtained (corresponding respectively to 0.15 to 0.3 mmol/g_{Pt}). This is comparable to the highest values usually reported in the literature for similar "grafting to" procedures performed on 2D and 3D inorganic substrates.[7,10] In addition, FTIR spectroscopy has been conducted to attest for the effective CuAAC "grafting to" reaction through the strong decrease of both the alkyne and azide signals in the spectrum of the resulting polymer-*grafted*-PtNPs (see Supporting Information).

Radii of gyration (R_g) of the polymer corona were precisely determined from SANS measurements (Figure 1) performed in deuterated dimethylacetamide (d_9-DMAc). The platinum core having the same neutron length density as d_9-DMAc, the scattering signal exclusively results from the hydrogenated polymer corona. SANS spectra of the different samples grafted with various polymer precursors, both showed a plateau at low q values and a decrease in $q^{-2.7}$ in the intermediate q range. This is typical of polymer star-shaped architecture usually obtained after polymer grafting on small inorganic core.[4d] At low q values, the intensity (I_0) increases with the M_n of the polymer precursors. R_g values of the polymer-*grafted*-PtNPs were determined using the Guinier approximation (see Supporting Information) and varied from 5.9 to 7.7 nm, as the size of the grafted chains increased (Table 1). Finally, TEM experiments (Figure 2) revealed the homogeneous size distribution of the platinum core and the nonaggregated state of the hybrid PtNPs. These examples have shown that the CuAAC "grafting to" process has been successfully conducted to functionalize PtNPs with biocompatible polymers.

Combined "Grafting From" ATRP and CuAAC "Grafting To" Strategies. Sequential combination of *surface*-ATRP and CuAAC "grafting to" approaches was then investigated in order to increase the complexity, the polymer corona density, and the chemical nature of the resulting hybrid PtNPs. This complementary approach relies on the *surface*-ATRP (co)polymerization of azide-functionalized monomers that affords a primary polymer corona with a higher quantity of azide functionalities compared to the previous approach, followed by the subsequent CuAAC "grafting to" process of ω-alkyne PEG and PCL chains (Scheme 2). This two- or three-step approach combines the integrative advantages of both the "grafting from" and "grafting to" methods and offers the potential to build up a wide library of PtNPs with tunable chemical nature, size, microstructure, density, and functionalities of the polymer corona.

First, random copolymerization of a 3:1 ratio of styrene and *p*-chloromethylstyrene (**1**) followed by nucleophilic substitution of the chloride groups by NaN_3 yielded PtNPs with azide-functionalized PS branches (PSN_3-*g*-PtNPs). No formation of hyperbranched polymers which may occur from ATRP has been observed, as the ratio of catalyst to

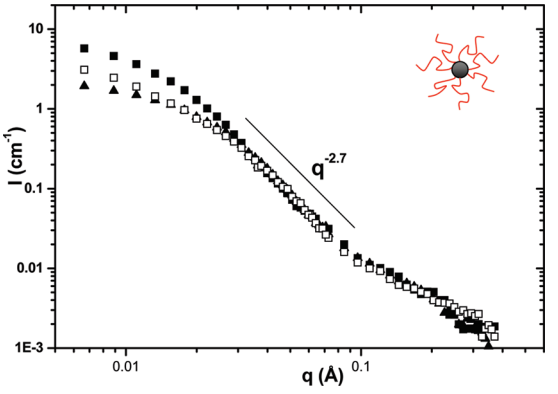

Figure 1. SANS spectra (d_9-DMAc, C = 6 mg/mL) of PCL-*g*-PtNPs (0.9 kg/mol, solid triangles), PCL-*g*-PtNPs (3 kg/mol, open squares), and PEG-*g*-PtNPs (solid squares) obtained by the CuAAC "grafting to" method.

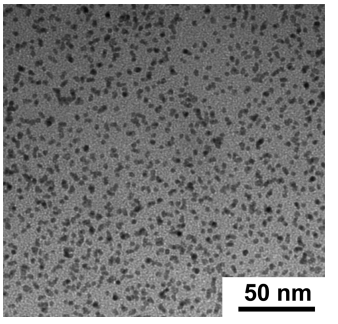

Figure 2. Transmission electron microscopy of PEG-*g*-PtNPs.

Table 1. Characteristics of the Polymer-*grafted*-PtNPs Obtained by the CuAAC "Grafting To" Approach

sample	M_n (kg/mol)	organic content (wt %)	n_{mol}/g_{Pt} (mmol/g_{Pt})	grafting rate (%)	grafting density (chain/nm^2)	R_g (nm)
N_3-PtNPs		18.6	0.37		2.7	
PCL-*g*-PtNPs	0.9	32.9	0.30	64.2	1.8	5.9
PCL-*g*-PtNPs	3.0	42.7	0.18	38.7	1.1	6.4
PEG-*g*-PtNPs	5.0	54.4	0.15	25.1	0.9	7.7

Table 2. Characteristics of the Hybrid PtNPs Obtained from the Combination of "Grafting From" *Surface*-ATRP and CuAAC "Grafting To" Approaches

sample	M_n (kg/mol)	polymer content (wt %)	n_{mol}/g_{Pt} (mmol/g_{Pt})	grafting rate (%)	R_g (nm)
PSN_3-*g*-PtNPs[a]		84.3	13		9.1
PCL/PS-*g*-PtNPs	0.9	89.4	3.4	39.6	10.5
PCL/PS-*g*-PtNPs	3.0	92.0	2	23.7	12.7
PEG/PS-*g*-PtNPs	5.0	91.7	1.1	7.6	13.0
$PBMAN_3$-*g*-PtNPs[a]		72.6	2.3		8.4
PCL/PBMA-*g*-PtNPs	0.9	77.0	0.8	32.9	10.0
PCL/PBMA-*g*-PtNPs	3.0	81.5	0.6	25.4	11.0
PEG/PBMA-*g*-PtNPs	5.0	84.0	0.5	22.5	11.5

[a] 25 mol % of azido-functionalized monomer.

Scheme 2. Construction of Hybrid PtNPs by Combination of ATRP "Grafting From" and CuAAC "Grafting To" Approaches

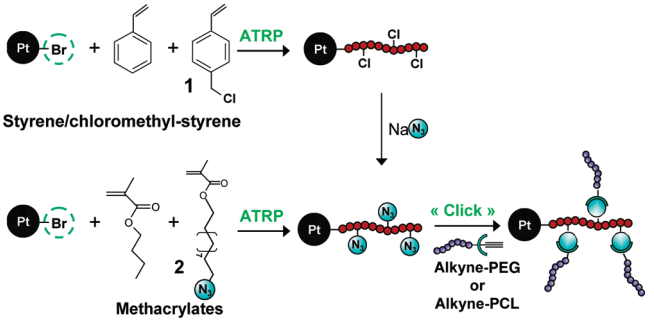

monomer was low.[11] Infrared spectra also clearly showed the presence of the chloride groups which then disappeared after conversion to azide groups (see Supporting Information). Second, random copolymerization of a 3:1 ratio of *n*-butyl methacrylate with a tailor-made azide-functionalized methacrylate (**2**) yielded in a single step PtNPs with azide-functionalized poly(*n*-butyl methacrylate) branches ($PBMAN_3$-*g*-Pt).[8a] Besides the advantages of the subsequent CuAAC "grafting to" process, the easy tuning of the number of click functionalities from the initial monomer ratio and the polymerization degree of the chains are the major benefits of this combined approach. Tailor-made ω-alkyne PEG and PCL described above were then grafted by CuAAC to the initial azide-functionalized copolymer branches.

The success of the grafting reactions was first evidenced by FTIR spectroscopy (see Supporting Information). Indeed, the characteristic signals of the alkyne functionalities from the linear precursors have disappeared, proving the effective removal of the unreacted polymer chains. In addition, the presence of the characteristic IR absorption bands of PEG or PCL together with the important decrease of the azide band confirms the successful grafting of polymer chains by CuAAC.

Compared to the initial CuAAC "grafting to" approach, the azide-functionalized PtNPs precursor contained a significantly higher amount of more accessible azide functionalities due to the presence of this first polymer layer (Table 2) with $M_n > 10$ kg/mol. In this combined method, we started with an azide-functionalized poly(*n*-butyl methacrylate) ($PBMAN_3$-*g*-Pt) layer with low monomer conversion (26%), i.e., short grafted chains. Nevertheless, the amount of azide units generated by this way at the surface of the particles is already 6 times higher than the molar amount involved in the previous CuAAC "grafting to" method (2.3 mmol of N_3/g of Pt, Table 2, compare to 0.37 mmol/g of Pt, Table 1). The grafting rates (efficiency) for a given polymer graft (same M_n) were comparable to those obtained by the "grafting to" approach, but still, the total amount of grafted chains per object is more than 3 times higher than the former CuAAC "grafting to" route. The grafting densities varied from 0.3 to 0.6 mmol of grafted polymer per gram of platinum. Interestingly, it appears that the difference is even more important with the highest M_n polymer precursors.

Subsequently, in order to increase the amount of initial azide moeties, we chose to (co)polymerize styrene and chloromethylstyrene, as the *surface*-ATRP from PtNPs of such monomers leads to higher conversion and therefore to higher amount of reacting sites.[4c,g] As summarized in Table 2, the number of initial azide functionalities, is 13 mmol/g of Pt, meaning 35 times more than for the functionalized particles used in the CuAAC "grafting to" procedure. For the 0.9 and 3 kg/mol PCL grafts, we succeeded in grafting 11 times more polymer chains than with the previous method (i.e., 3.4 and 2 mmol/g of Pt, respectively).

Therefore, this combination of "grafting from" and "grafting to" techniques, not only permits to vary the nature of the sequential polymer layer but also leads to a higher grafting density of "clicked chains" per object. This could be explained by a better accessibility of the further grafted chains toward the initial solubilized polymer layer, rather than to the small compact core of PtNPs. This is coherent with what is usually observed in the literature where grafting densities from organic substrates usually show higher grafting densities than from inorganic ones.[12]

The formation of a much denser polymer corona has also been verified by SANS. The SANS spectra obtained from the "clicked" hybrid PtNPs (by combination of "grafting from" and "grafting to" method), and from its polymer-*grafted* precursor, are reported in Figure 3.

For the copolymer-*grafted*-PtNPs (the hybrid precursor), the SANS signal is typical of a polymer layer obtained from the *surface*-ATRP from PtNPs (star-shaped structure).[4d] At low q values, a plateau is observed. Again, R_g of the objects could be estimated using the Guinier approximation. After the CuAAC grafting of PEG chains, the intensity at low q increases significantly, meaning that the scattering polymer

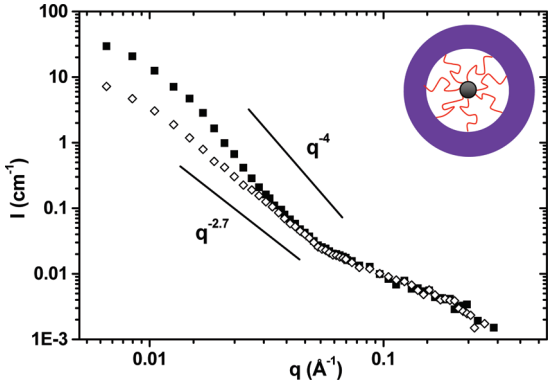

Figure 3. SANS spectra (d_9-DMAc, C = 6 mg/mL) of PtNPs grafted with copolymers based on styrene precursor (open diamonds) and "clicked" with PEG 5 kg/mol (solid squares).

layer is more important. The other important difference relies on the decrease of the signal in the intermediate q range. As mentioned before, the first layer gives a typical star-shaped corona with a decrease in $q^{-2.7}$ as for the previously discussed "grafting to" approach. However, after subsequent click chemistry, the decrease of the signal of the "click" layer is closer to a Porod law in q^{-4}. This confirms the transition from a smooth to a sharper interface, meaning that the grafting density of the polymer corona significantly increases after the second grafting procedure.

Conclusion

Consequently, we presented two efficient methods to graft PEG or PCL chains onto PtNPs via click chemistry. The first one involving the direct CuAAC "grafting to" of ω-alkyne PCL or PEG onto previously azide-functionnalized PtNPs, was efficient and easy to perform. The second one, including a combination of *surface*-ATRP and CuAAC, is a powerful technique which combines the merits of both "grafting to" and "grafting from" approaches in terms of chemical nature and microstructure of the resulting polymer layer. In addition, quantitative analysis from TGA and SANS studies showed that the grafting density per object strongly increased when using this combined method, compared to the classical "grafting to" approach based on CuAAC reaction. Given the modular nature of these reactions and the broad array of polymer architectures accessible (hydrophilic, hydrophobic, amphiphilic, neutral, charged, functionalized, etc.), these general methodologies could be useful for the preparation of more complex and tunable materials based on tailor-made functionalized PtNPs or other metal nanoparticles, from easily accessible end-functionalized click polymers. Our interest in such architectures is based on the electrochemical properties of the nanostructures and their usefulness in biodetection, as will be shown in a forthcoming paper.

Acknowledgment. The authors gratefully acknowledge the financial support from the Agence Nationale de la Recherche under Contract ANR-07-JCJC-0020 [MULTICLICK]. We also thank Dr. Christopher J. Plummer (EPFL, Lausanne, CH) for his help with TEM measurements.

Supporting Information Available: Characterization (FTIR spectroscopy) for the intermediates and hybrid polymer-*grafted*-PtNPs, *surface*-ATRP kinetics, calculation of grafting rates and grafting densities, and SANS data treatments. This material is available free of charge via the Internet at http://pubs.acs.org.

References and Notes

(1) (a) Stamenkovic, R. S.; Fowler, B.; Mun, B. S.; Wang, G.; Ross, P. N.; Lucas, C. A.; Markovic, N. M. *Science* **2007**, *315*, 493–497. (b) Tian, N.; Zhou, Z. Y.; Sun, S. G.; Ding, Y.; Wang, Z. L. *Science* **2007**, *316*, 732–735. (c) Chen, A.; Holt-Hindle, P. *Chem. Rev.* **2010**, *110*, 3767–3804.

(2) (a) Guo, S.; Dong, S. *Trends Anal. Chem.* **2009**, *28*, 96–109. (b) Pang, X.; He, D.; Luo, S.; Cai, Q. *Sens. Actuators, B* **2009**, *137*, 134–138. (c) Bashbi, L.; Fransconi, M.; Tel-Vered, R.; Yehezkeli, O.; Willner, I. *Anal. Chem.* **2008**, *80*, 8253–8259. (d) Shang, F.; Glennon, J. D.; Luong, J. H. T. *J. Phys. Chem. C* **2008**, *112*, 20258–20263.

(3) (a) Radhakrishnan, B.; Ranjan, R.; Brittain, W. J. *Soft Matter* **2006**, *2*, 386–396. (b) Matyjaszewski, K.; Tsarevski, N. V. *Nature Chem.* **2010**, *1*, 276–288.

(4) (a) Perez, H.; Pradeau, J. P.; Albouy, P. A. *Chem. Mater.* **1999**, *11*, 3460–3463. (b) Perez, H.; Noël, V.; Etcheberry, A.; Cavalière-Jaricot, S.; Albouy, P. A. *Thin Solid Films* **2008**, *517*, 755–763. (c) Carrot, G.; Perez, H. *Polym. Prepr.* **2006**, *43*, 827–828. (d) Carrot, G.; Gal, F.; Cremona, C.; Vinas, J.; Perez, H. *Langmuir* **2009**, *25*, 471–478. (e) Cavaliere, S.; Raynal, F.; Etcheberry, A.; Herlem, M.; Perez, H. *Electrochem. Solid State Lett.* **2004**, *7*, A358–A360. (f) Cavalière-Jaricot, S.; Haccoun, J.; Etcheberry, A.; Herlem, M.; Perez, H. *Electrochim. Acta* **2008**, *53*, 5992–5999. (g) Al Akhrass, S.; Gal, F.; Damiron, D.; Alcouffe, P.; Hawker, C. J.; Cousin, F.; Carrot, G.; Drockenmuller, E. *Soft Matter* **2009**, *5*, 586–592.

(5) (a) Rostovtsev, V. V.; Green, L. G.; Fokin, V. V.; Sharpless, K. B. *Angew. Chem., Int. Ed.* **2002**, *41*, 2596–2599. (b) Tornoe, C. W.; Christensen, C.; Meldal, M. *J. Org. Chem.* **2002**, *67*, 3057–3064.

(6) (a) Lutz, J.-F. *Angew. Chem., Int. Ed.* **2007**, *46*, 1018–1025. (b) Mynar, J. L.; Choi, T. L.; Yoshida, M.; Kim, V.; Hawker, C. J.; Frechet, J. M. J. *Chem. Commun.* **2005**, *41*, 5169–5171. (c) Meldal, M.; Tornoe, C. W. *Chem. Rev.* **2008**, *108*, 2952–3015. (d) Iha, R. K.; Wooley, K. L.; Nystrom, A. M.; Burke, D. J.; Kade, M. J.; Hawker, C. J. *Chem. Rev.* **2009**, *109*, 5620–5686.

(7) (a) Ostaci, R.-V.; Damiron, D.; Capponi, S.; Vignaud, G.; Léger, L.; Grohens, Y.; Drockenmuller, E. *Langmuir* **2008**, *24*, 2732–2739. (b) Sommer, W. J.; Weck, M. *Langmuir* **2007**, *23*, 11991–11995. (c) Gehan, H.; Fillaud, L.; Felidj, N.; Aubard, J.; Lang, P.; Chehimi, M. M.; Mangeney, C. *Langmuir* **2010**, *26*, 3975–3980. (d) Such, G. K.; Quinn, J. F.; Quinn, A.; Tjipto, E.; Caruso, F. *J. Am. Chem. Soc.* **2006**, *128*, 9318–9319. (e) Ranjan, R.; Brittain, W. J. *Macromolecules* **2007**, *40*, 6217–6223. (f) Ranjan, R.; Brittain, W. J. *Macromol. Rapid Commun.* **2007**, *28*, 2084–2089. (g) Ranjan, R.; Brittain, W. J. *Macromol. Rapid Commun.* **2008**, *29*, 1104–1110. (h) Campidelli, S.; Ballesteros, B.; Filoramo, A.; Díaz Díaz, D.; Torres, T.; de la Torre, G.; Rahman, G. M. A.; Ehli, C.; Kiessling, D.; Werner, F.; Sgobba, V.; Guldi, D. M.; Cioffi, C.; Prato, M.; Bourgoin, J.-P. *J. Am. Chem. Soc.* **2008**, *130*, 11509–11509. (i) Boisselier, E.; Salmon, L.; Ruiz, J.; Astruc, D. *Chem. Commun.* **2008**, *44*, 5788–5790.

(8) (a) Damiron, D.; Desorme, M.; Ostaci, R.-V.; Al Akhrass, S.; Hamaide, T.; Drockenmuller, E. *J. Polym. Sci., Part A: Polym. Chem.* **2009**, *47*, 3803–3813. (b) Malkoch, M.; Schleicher, K.; Drockenmuller, E.; Hawker, C. J.; Russell, T. P.; Wu, P.; Fokin, V. V. *Macromolecules* **2005**, *38*, 3663–3678. (c) Colinet, I.; Dulong, V.; Hamaide, T.; Le Cerf, D.; Picton, L. *Carbohydr. Polym.* **2009**, *75*, 454–462.

(9) (a) Lindner, P. In *Neutrons, X-ray and Light Scattering Methods Applied to Soft Condensed Matter*; Lindner, P., Zemb, T., Eds.; North-Holland: Amsterdam, 2002; Chapter 2, p 23. (b) Brûlet, A.; Lairez, D.; Lapp, A.; Cotton, J.-P. *J. Appl. Cryst.* **2007**, *40*, 165–177.

(10) Wang, B.; Li, B.; Zhao, B.; Li, C. Y. *J. Am. Chem. Soc.* **2008**, *130*, 11594–11595.

(11) Weimer, M. W.; Frechet, J. M. J.; Gitsov, I. *J. Polym. Sci., Part A: Polym. Chem.* **1998**, *36*, 955–970.

(12) (a) Ostaci, R. V.; Damiron, D.; Grohens, Y.; Léger, L.; Drockenmuller, E. *Langmuir* **2010**, *26*, 1304–1310. (b) Nebhani, L.; Schmiedl, D.; Barner, L.; Barner-Kowollik, C. *Adv. Funct. Mater.* **2010**, *20*, 2010–2020.